IMPACT OF COMPONENT TERMINAL FINISH ON THE RELIABILITY OF Pb-FREE SOLDER JOINTS

Gregory Henshall, Patrick Roubaud, Geary Chew
Hewlett-Packard Co.
Palo Alto, California
greg_henshall@hp.com

Swaminath Prasad, Flynn Carson
ChipPAC Inc.
Fremont, California

Eamon O'Keeffe
Sanmina-SCI Corporation
San Jose, California

Ronald Bulwith
Alpha Metals Inc.
Cookson Electronics Assembly Materials
Jersey City, New Jersey

ABSTRACT

The transition to Pb-free electronics has prompted the development of Pb-free component terminal finishes. Among the candidates being investigated are pure tin and dilute alloys of tin with either bismuth or copper. Of course, reliability of the solder joints made between the Pb-free Sn-Ag-Cu alloy and these component terminal finishes is essential. Metallurgical incompatibility between the Sn-Ag-Cu solder alloy and the terminal finishes could result in solder joint brittleness, low strength or lack of thermal fatigue resistance, particularly following aging of the joint (e.g. over the life of a product in the field).

In this study, we investigated the reliability of SMT solder joints made with Sn-3.8Ag-0.7Cu solder and leaded components with a variety of surface finishes: pure Sn, Sn-3Cu, and Sn alloyed with Bi in concentrations of 1, 3 and 6 weight percent. This investigation included metallographic examination and lead pull testing of aged and unaged joints. Accelerated thermal cycling of surface mount joints also has been initiated and preliminary results are described. The results of a limited study on the quality of wave soldered, through-hole joints with Sn-Bi and Sn-Pb platings are also presented. Our findings suggest that all of the Pb-free terminal finishes investigated produce joints with Sn-Ag-Cu solder that perform at least as well as conventional, fully Sn-Pb joints.

Key words: Pb-free solder, terminal finish, reliability

INTRODUCTION

It is almost certain that European legislation will ban the intentional use of lead in most electronic products by January 1, 2006. In addition, many Japanese original equipment manufacturers (OEMs) have transitioned a small part of their product volume to be Pb free, or at least to include Pb-free solder processes. As a result, the electronic components industry has been investigating Pb-free alternatives to the Sn-Pb terminal platings commonly used in today's electronic products. Some suppliers have actually begun offering Pb-free lead platings for their leaded packages.

Among the candidate terminal platings being investigated (or sold) are pure tin and dilute alloys of tin with bismuth or copper. An important requirement of any new lead finish is good reliability of the solder joints made between it and the Sn-Ag-Cu alloy most of the industry is planning to use for Pb-free printed circuit assemblies (PCAs). Metallurgical incompatibility between the Sn-Ag-Cu solder alloy and the terminal finishes could result in solder joint brittleness, low strength or lack of thermal fatigue resistance, particularly following aging of the joint (e.g. over the life of a product in the field).

For through-hole joints, the concern over reliability of a "well formed" joint is low. However, there is concern that obtaining complete barrel fill and wetting the solder to the pin may be more difficult with the Pb-free materials than with conventional Sn-Pb solders and lead platings. It is also less clear which solder alloy(s) the industry will ultimately converge upon for volume manufacturing of wave soldered through-hole joints. Sn-0.7Cu (all alloy compositions are given in weight percent) and Sn-Ag-Cu are currently candidates.

In this study, we investigated the reliability of SMT solder joints made with Sn-3.8Ag-0.7Cu solder and leaded components with surface finishes of pure matte Sn, Sn-3Cu, and Sn alloyed with Bi in concentrations of 1, 3, and 6 weight percent. These are among the common finishes being considered in the electronics industry as replacements for Sn-Pb. This investigation included metallographic examination and lead pull testing of aged and unaged joints. Accelerated thermal cycling of surface mount joints also has been initiated.

For plated through-hole (PTH) joints, we studied fillet shape and wetting of the solder to the lead. Investigation of PTH joints was made for two lead finishes, Sn-10Pb and Sn-3Bi, and for two Pb-free solder alloys, Sn-4.0Ag-0.5Cu and Sn-0.7Cu. Results of the wetting and barrel fill analyses were compared to those from control joints using Sn-Pb plating and eutectic Sn-Pb solder.

EXPERIMENTAL MATERIALS AND PROCEDURES
Test Vehicle
The SMT experiments were performed on test assemblies employing a double-sided printed circuit board (PCB) designed especially for this investigation. The top side of the board (side A) was used to test six SMT package types: TSOP-32, MQFP-208, PBGA-388, PLCC-32, SOIC-8, Tape CSP-48. The bottom side (side B) had eight locations, four for the MQFP-208 and four for the SOIC-8 packages. The lead frame alloy for the MQFPs studied in detail here was copper C7025. The board design details are provided in Table 1.

PCB Dimensions	203 x 145 mm
PCB thickness	62 mils
PCB layers	4
PCB pad design	Non solder mask defined
PCB pad finish	OSP copper

Table 1. Features of the SMT board design.

The PCBs to be used in lead-free products employing Sn-Ag-Cu solders will have to withstand the associated high reflow temperatures, thereby imposing a higher stress on the board layers. For this reason the standard FR-4 board was not used for the experiments. Instead, a polyclad material was used as a base. The coating on the copper pads consisted of organic solderability preservative (OSP).

Assembly of SMT components was performed at the Sanmina-SCI facility in San Jose, California. The Pb-free PCAs were assembled with the Sn-3.8Ag-0.7Cu (SAC) solder. The maximum reflow temperature on the board reached 245 °C for the top (side A) and 250 °C for the bottom (side B), as measured on the PCB. Maximum component temperatures were slightly lower, ranging from 237 – 245 °C. Time over the solder melting point of 217 °C ranged from 46 – 70 s, depending on location. The control boards were assembled with eutectic Sn-37Pb solder using conventional methods.

The PTH components were assembled separately at the Cookson-Speedline facility in Camdenton, Missouri. Wave soldering was performed on Ni/Au-coated PCBs with one PDIP-24 component on each board. Alphametals NR 330 flux was used with eutectic Sn-Pb control and two Pb-free solders: Sn-4.0Ag-0.5Cu and Sn-0.7Cu. The solder bath temperature was 260 – 273 °C. The leads of the PDIP-24 packages were coated with either a conventional Sn-10Pb plating or with a Sn-3Bi plating. 10 assemblies with each solder/plating combination were manufactured. Some non-wetting was observed on the Ni/Au-coated PCB pads but no evidence of non-wetting of the leads was observed during manufacturing.

Aging and Microstructural Analysis
Aging of the SMT joints was performed to accelerate the conditions that typical solder joints may be subjected to during their service life. The goal was to see what changes to the solder joint microstructure and, especially, the intermetallic layer thicknesses, take place over time at elevated temperature. This information was then combined with the mechanical test data to provide an understanding of how the various lead platings influence the long-term reliability of SMT joints.

Aging of the SMT assemblies was performed in air. The aging was performed at temperatures of 125 °C, 150 °C and 175 °C for times of 1, 2, 4, 8, 16, and 32 days. Analysis of the effect of aging on solder joint microstructure was performed only on the MQFP-208 packages, which are assumed to be representative of the other leaded packages. One or two leads from unaged packages or those aged at each temperature for 4, 8, and 32 days were examined for the analysis presented later in this paper. The joint metallurgies examined include: Sn-37Pb solder with Sn-10Pb plating (SnPb/SnPb), Sn-3.8Ag-0.7Cu solder with matte Sn plating (SAC/Sn), Sn-3.8Ag-0.7Cu solder with Sn-3Bi plating (SAC/SnBi), and Sn-3.8Ag-0.7Cu solder with Sn-3Cu plating (SAC/SnCu). The impact of aging on array packages was not included in this study but has been reported for PBGA-388 packages elsewhere by the authors [1].

Lead Pull
Pulling of the SMT leads from the PCB was used to measure the strength of the joints for each of the lead platings investigated. The impact of aging on lead pull strength was also studied. To keep the scope manageable, this investigation was performed only on the QFP-208 packages in the unaged condition and after aging 8 days at 125, 150 and 175 °C.

To accomplish the lead pull, the package body was first removed from the leads. This process was performed using a machinists mill and a small, circular diamond saw to ensure consistent cutting of the leads from the package body in a way that did not damage the joints. Lead pull testing was performed on an Instron Model 8848 microtester. A specially prepared pair of pneumatically-actuated needle-

nose pliers was used to grip each lead for pull testing. Fig. 1 shows the experimental set-up used for pull testing. 20 leads were pulled for each package to provide a statistical distribution of joint strengths. Each lead was pulled orthogonal to the surface of the PCB at a fixed displacement rate of 0.25 mm/min. Load and crosshead displacement data were collected on a PC and analyzed to provide the maximum load and the extension at failure for each lead. Selected fracture surfaces were examined in a JEOL Model JSM-IC848A scanning electron microscope (SEM).
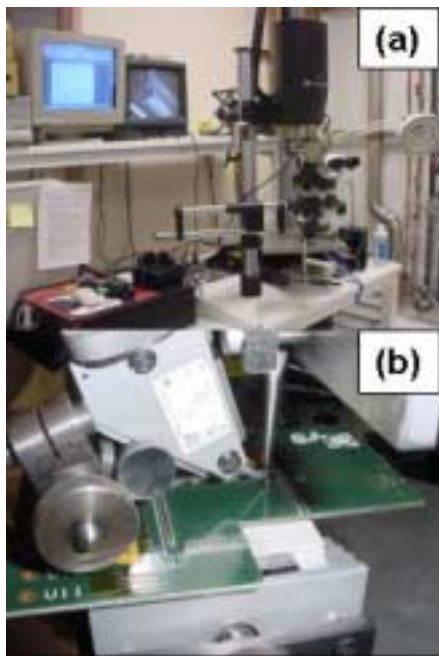
Figure 1. Experimental set-up for lead pull testing.

Accelerated Thermal Cycling
To investigate the resistance of the SMT solder joints to thermal fatigue, accelerated thermal cycle (ATC) testing was performed. The accelerated cycle conditions were: -40 °C to +125 °C with a 60 minute cycle (15 minute ramps and dwells). A sample size of 24 for each package type was selected to provide a reasonably accurate determination of the Weibull slope and characteristic life (defined as 63% failure) while keeping the test size manageable. Each of the components had a single daisy chain and was considered to fail when the daisy-chain resistance rose above a critical value. Thermotron$^{®}$ temperature chambers equipped with Hewlett-Packard E1346A data acquisition systems were used for continuous monitoring of the daisy chain resistances.

EXPERIMENTAL RESULTS AND DISCUSSION
Joint Microstructure and Intermetallic Growth
The as-assembled microstructures were consistent with what has been previously reported [1,2], both for the Sn-Pb and Pb-free joints. The Sn-Pb joints exhibited thin intermetallic layers at the interface with both the PCB pad and the component leads. These IMC layers had a "scalloped" shape [2] and a thickness of approximately 1.5 – 1.6 µm. Figure 2 shows a typical example of the microstructure of

the as-assembled Pb-free joints. Note the highly irregular, scalloped interface between the intermetallic compound (IMC) and the SAC solder. Also typical of all the as-assembled microstructures is that only the Cu_6Sn_5 phase is visible. Compared to SnPb joints, the SAC joints had somewhat thicker PCB/solder intermetallic layers in the as-assembled conditions, 2.3 – 2.9 µm, which is consistent with an earlier study [1]. There was a greater dependence of IMC thickness on the plating alloy at the lead/solder interface than at the PCB/solder interface. The IMC thickness ranged from 1.6 µm for the Sn-coated leads to 3.2 µm for the SnCu-coated leads.
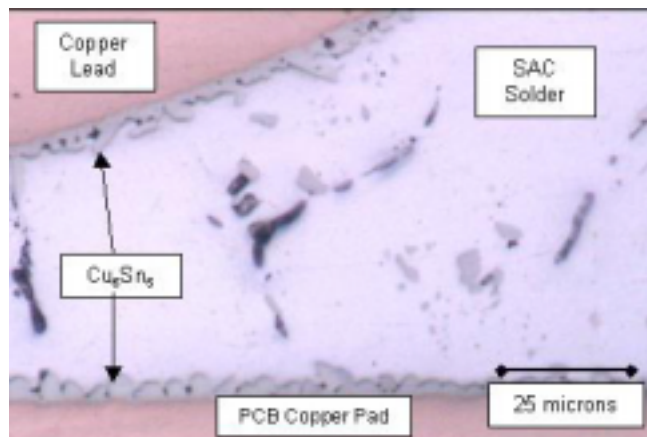
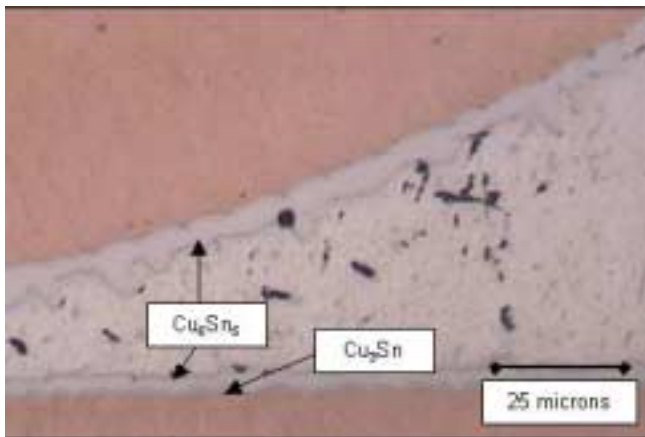**Figure 2**. Microstructure of a SAC/SnCu joint in the as-assembled condition.
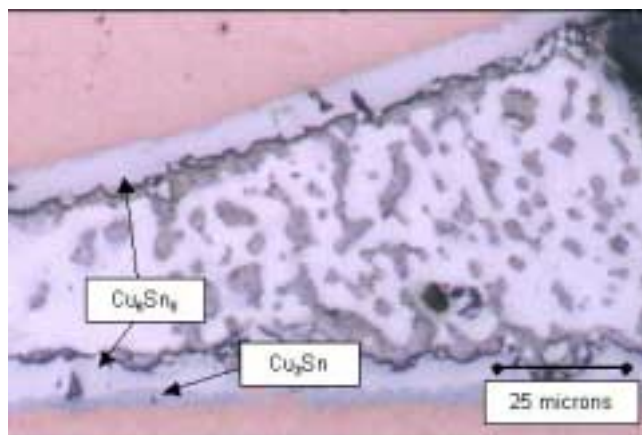
**Figure 3**. Microstructure of a SnPb/SnPb joint following aging at 175 °C for 4 days.

Aging of the Sn-Pb joints produced growth of the intermetallic layer in a way typical of what has been reported by others [1-3]. Specifically, at the PCB interface, the Cu_3Sn phase becomes apparent between the copper pad and the Cu_6Sn_5 phase, Figure 3. (Note: independent verification of these phase compositions was not made in this investigation. Rather, they were inferred from the Cu-Sn phase diagram and from earlier studies [2,3].) Since this behavior has been well documented [2,3], no attempt was made to measure the two layers separately. All IMC

thickness measurements were made to include both layers (if both were present). Interestingly, the Cu_3Sn phase did not become apparent at the lead/solder interface under any of the aging conditions. IMC growth at this interface was also somewhat less than at the PCB interface for the SnPb/SnPb joints. This difference may be due to the fact that the SAC joints are at a lower homologous temperature than the SnPb joints for any given aging condition. Also note that for both locations, the interface between the Cu_6Sn_5 and the solder remained rough but the scalloped appearance diminished as the layers became thicker.

Growth of the intermetallic compounds in the Pb-free joints was somewhat more complex than in the Sn-Pb joints. Figure 4 illustrates a typical microstructure for the aged Pb-free joints. At the PCB interface, the total IMC growth rate (including both Cu_3Sn and Cu_5Sn_6) appears to be slightly less than in the Sn-Pb joints. This finding is illustrated by the data given in Figure 5 for the intermediate aging temperature of 150 °C.


**Figure 4**. Microstructure of a SAC/Sn joint following aging at 150 °C for 8 days.
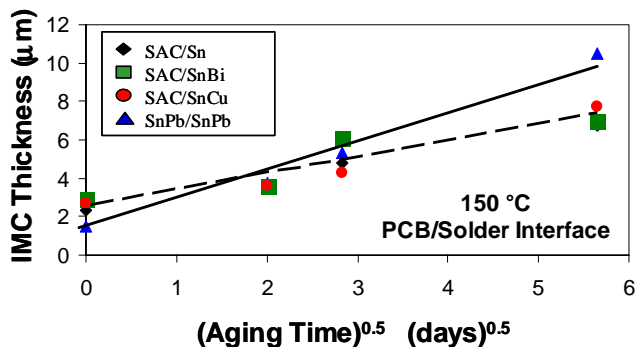
Figure 5. Total intermetallic layer thickness at the PCB/solder interface as a function of aging time at 150 °C.

At the component lead/solder interface, the IMC growth rate varied among the different Pb-free alloys, as shown in Fig. 6. The IMC growth rate for the SAC/Sn and SAC/SnCu joints was similar to that for the SnPb/SnPb joints. The growth rate for the SAC/SnBi joints was slightly larger than

for the other joints for intermediate aging treatments, and then became much larger for severe aging conditions (e.g. 150 °C for 32 days and 175 °C for 8 days). In fact, the IMC layer became so thick at the most extreme aging treatments that cracks formed in the layer, Fig. 7. It is not known whether these cracks were formed during aging or during preparation of the metallographic sample, but they are an indication that the IMC layer is brittle when it becomes thick. Cracks in the Sn-Bi coating at the bend of unassembled QFP leads have also been observed by Schroeder [6]. The reason for the higher growth rate in the SAC/SnBi joints after severe aging is not known. Microchemical analysis performed in the scanning electron microscope (SEM) did not reveal any Bi within the layer. One possible reason for the high growth rate is that Bi in the Sn solid solution increases the diffusion rate of Cu, and thus increases the rate of IMC growth. Resolution of this issue, however, was beyond the scope of this investigation.
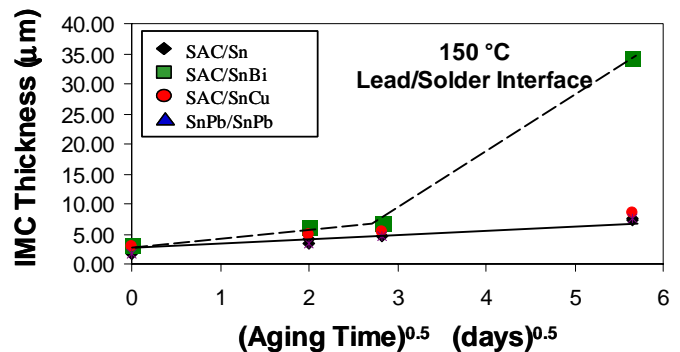
Figure 6. Total intermetallic layer thickness at the component lead/solder interface as a function of aging time at 150 °C.
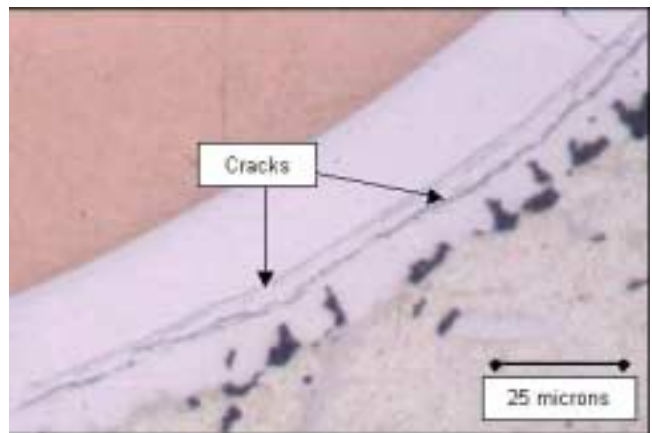
Figure 7. Cracks in the IMC layer for a SAC/Sn3Bi joint aged at 150 °C for 32 days. The thickness of this layer is approximately 34 μm.

Based on the data generated in this investigation, estimates of the IMC growth kinetics can be made. Since only three temperatures were studied and the aging time was limited to 32 days, this study does not constitute an exhaustive

investigation of IMC growth kinetics in Pb-free joints. Thus, the results obtained here must be considered estimates.

Following the work of Vianco, et al. [3], it was assumed that the total IMC growth rate follows the equation:

$$w(t) = w_o + A\, t^{\,n} \exp(-Q/RT) \qquad (1)$$

where $w(t)$ is the total IMC layer thickness at time t, w_o is the initial thickness, A is a constant, n is the time exponent of the growth rate, Q is the apparent activation energy for growth, R is the universal gas constant, and T is the aging temperature in Kelvin. As shown in Figs. 5 and 6, the data generated in this study suggest that making the assumption $n = \frac{1}{2}$ (diffusion-controlled growth) is reasonable, except for the Sn-Bi lead finish at long aging times. Solving eqn. (1) for the growth rate as a function of T at constant aging time gives:

$$\ln[w(t^*) - w_o] = \ln[A(t^*)^n] - (Q/R)(1/T) \qquad (2)$$

where t^* denotes that t is held constant for this analysis. This equation indicates that a plot of the natural logarithm of the change in IMC thickness as a function of $1/T$ should yield a straight line of slope $-(Q/R)$. Figure 8 shows an example of such a plot for SAC/Sn joints aged 8 days at a range of temperatures. The values of Q for total IMC growth at the PCB/solder and component lead/solder interfaces are given in Table 2.
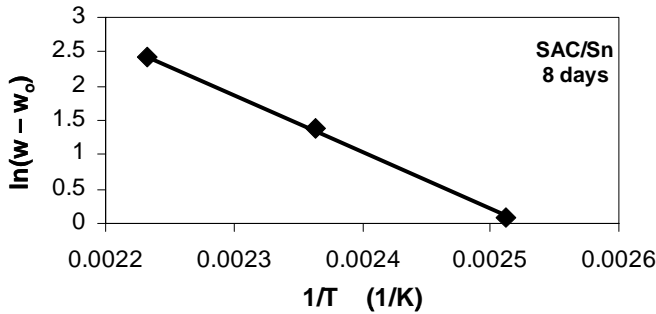
Figure 8. Data for IMC growth on the lead of a SAC/Sn joint aged for 8 days plotted to reveal the apparent activation energy for IMC growth, Q.

Solder Alloy	Lead Finish Alloy	PCB/Solder Q (kJ/mol)	Lead/Solder Q (kJ/mol)
SnPb	SnPb	65	68
SAC	Sn	68	69
SAC	Sn3Bi	97	137
SAC	SnCu	79	109

Table 2. Apparent activation energy results.

The value of Q for the Sn-Pb joints is essentially the same for both interfaces. The value of 65 – 68 kJ/mol is somewhat higher than the value of 45 kJ/mol measured

earlier by the authors [1] and by Vianco et al. [3]. The apparent activation energy measured for the SAC/Sn joints is very similar to that for the Sn-Pb joints, both in magnitude and in the fact that it is essentially the same for both interfaces. This is not the case for the other two Pb-free joints. For the SAC/SnCu joints, Q at the PCB/solder interface is about 20% higher than for the SAC/Sn or SnPb/SnPb joints. Given the difficulty in making thickness measurements, this difference may be due to experimental error. The value of Q for the lead/solder interface is about 60% larger than the corresponding value for the SAC/Sn. It is unlikely that this difference is due to experimental error. For the SAC/SnBi joints, the activation energies are even larger. At the PCB/solder interface, Q is about 50% larger for the SAC/SnBi joints than for the SAC/Sn or SnPb/SnPb joints. At the component lead/solder interface, Q for the Bi-containing joints is about twice that of the SnPb/SnPb or SAC/Sn joints. These large differences are consistent with the remarkably different growth rates observed for the SAC/SnBi joints shown in Fig. 6. At this time, it is not clear why the activation energies for total IMC growth vary depending on the joint metallurgy. It is noteworthy, however, that the Sn-3Bi and Sn-3Cu surfaces are much rougher than the matte Sn and Sn-10Pb surfaces prior to assembly [6], suggesting that diffusion may be more rapid at these surfaces. Clearly, this issue warrants further study.

Lead Pull Strength

The impact of the microstructural changes, particularly the IMC thickness, on the strength of the QFP solder joints was investigated by lead pull testing. Joints were tested in the unaged condition and after aging 8 days at 125, 150, and 175 °C.

Three types of failure modes were observed, as illustrated in Fig. 9(a). Type 1 failures were characterized by a monotonic increase in load, P, with increasing displacement, δ. The lead then separated from the solder suddenly, and the load dropped to zero. Type 2 failures, which were most common for the 150 °C aging treatment, had a more complex shape. For this mode, P initially rose with increasing δ, then dropped to an intermediate "plateau" prior to final fracture. Observation of Type 2 failures showed that the initial drop in P was associated with fracture at the heel of the joint. During the plateau, a crack continued to propagate near the lead/solder interface until it reached the toe and the load dropped to zero. Type 3 failures were characterized by low loads, low displacements and a P – δ curve in which the load peaked prior to final fracture. For all three failure modes, fracture occurred near the lead/solder interface, never near the solder/PCB pad interface. Finally, in cases where peak loads were high, pads occasionally pulled out of the polyclad. These pull-out failures were not used in the analysis of lead pull behavior.

It has been shown in previous work [4] that P_{max} alone is not the best indicator of the mechanical integrity of a joint in lead pull testing. The energy required to fracture the joint, or the "toughness," is another key parameter. Therefore,

we have estimated the toughness of the joints for Type 1 failures as shown in Fig. 9(b). Rigorously, the toughness is given by the area under the true stress – true strain curve, which would be difficult to assess given the complex geometry of the joints. However, assuming the joints have a relatively consistent geometry, the toughness is proportional to the area under the $P – \delta$ curve. To simplify the measurement of toughness further, we estimated this area only for Type 1 failures. As shown in Fig. 9(b), this was accomplished by calculating the area of the triangle defined by P_{max} and the displacement at failure, δ_{max}. Examination of the $P – \delta$ curves showed that this methods underestimates the area consistently by about 20% but should provide for a comparison among the different solder joint metallurgies and aging treatments. Furthermore, we report here the average toughness for many individual leads (up to 20, depending on how many Type 1 failures occurred). For Type 2 and Type 3 failures, no effort was made to measure the area under the $P – \delta$ curves but both the peak load and displacement at failure are reported.
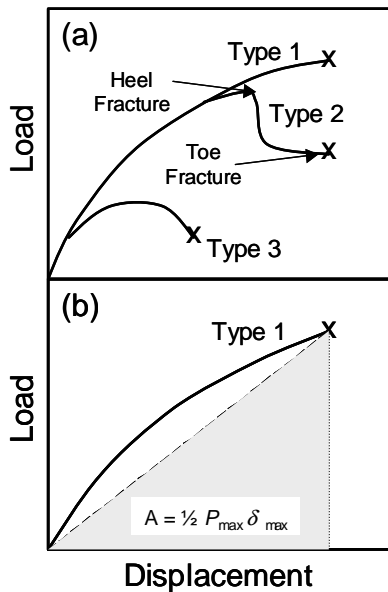

Figure 9. Schematic illustrations of (a) the three failure modes observed and (b) the method used to estimate toughness for Type 1 failures.

Figure 10(a) shows the average P_{max} values for Type 1 failures only. Data for each type of joint studied are given as a function of aging treatment. The standard deviation in peak load was small, approximately corresponding to the height of the plotting symbols, so "error bars" are omitted for clarity. The key finding is that the SAC joints are as strong or stronger than the SnPb/SnPb joints under all aging conditions up to 175 °C, where the IMC layers become quite thick, on the order of 10 μm or greater. Thus, these data suggest that aging of the joints has minimal impact on the strength of the joint until the IMC layer becomes quite thick. For example, the data at 150 °C show that the joints maintain their strength relative to the as-assembled values and that the Pb-free joints remain stronger than the

SnPb/SnPb joints. IMC layer thicknesses in this case are 4.5 – 7 μm.

Figure 10(b) presents the estimated toughness data for Type 1 failures only. There is greater scatter in the δ_{max} data than the P_{max} data, so the estimated toughness plot shows more scatter than is shown in Fig. 10(a). Standard deviation "error bars" are given for the 150 °C data as an indication of this scatter. There was a similar amount of scatter for the unaged joints and for those aged at 125 °C (error bars omitted for clarity). Again, in the unaged condition the toughness of the Pb-free joints is greater than or equal to that of the SnPb/SnPb joints. These toughness values are maintained up to the 150 °C aging treatment, at which point the IMC layers are 4.5 – 7 μm thick compared to 2 – 3 μm in the as-assembled condition. The Pb-free joints show estimated toughness values equal to or greater than those for the SnPb joints up to and including the 150 °C aging treatment. The exception to this is the SAC/SnCu joint aged at 125 and 150 °C, which is likely a result of scatter in the data. Consistent with the P_{max} data, the toughness values fall significantly for all the joint types for the 175 °C aging treatment. In this case, the IMC thickness ranges from 10 – 20 μm. It is unlikely that joints in service would ever grow IMC layers this thick since products are typically specified to operate at temperatures below 50 – 70 °C, depending on the type of product. In addition, 175 °C corresponds to a homologous temperature of 0.914, and such high temperatures may activate mechanisms not relevant for those at which products operate in service.
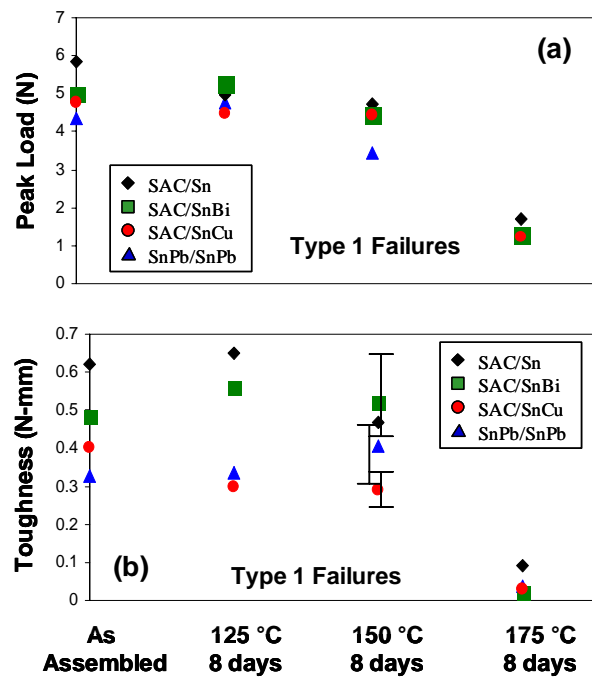
Figure 10. For Type 1 failures only, the maximum load (a) and estimated toughness (b) of QFP solder joints subjected to four different aging conditions.

If we include all the failure modes in the analysis, the trends described above are mostly unchanged. Figure 11 presents the maximum load and failure displacement data as a weighted average from all three failure modes. Figure 11(a) shows some evidence for a small drop in P_{max} for the 150 °C aging condition that was not as evident in the Type 1 data. Compared to the unaged conditions, P_{max} has dropped between 15% (SAC/SnCu) and 40% (SAC/SnBi). Still, within experimental error, the Pb-free joints show strengths greater than or equal to that of the SnPb joints for all aging conditions. The failure displacement data exhibit considerable scatter. However, it appears clear that δ_{max} stays relatively constant for aging treatments up to 150 °C for 8 days and then drops significantly for the 175 °C aging. This is consistent with the strength and toughness data, and suggests that there may be a critical IMC layer thickness above which fractures become brittle and are associated with low loads and displacements.
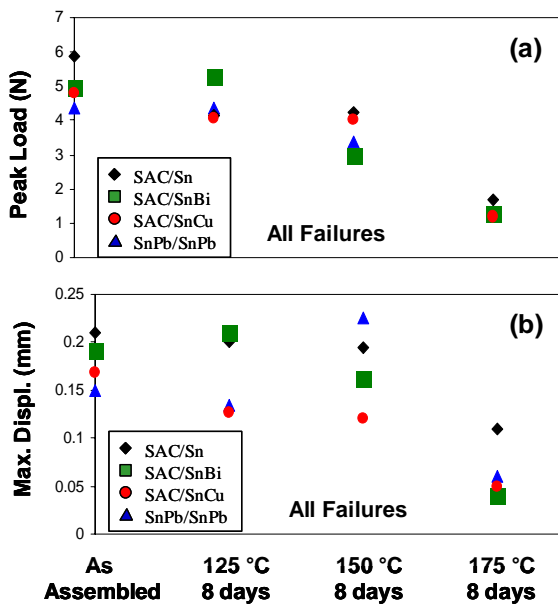

Figure 11. For all failures types, the weighted average of the maximum load (a) and (b) maximum displacement of QFP solder joints subjected to four different aging conditions.

A limited investigation of the fracture surfaces using SEM was undertaken to correlate the mechanical data with the characteristics of the fracture surface. All fractures took place near the lead/solder interface (as opposed to the lead/PCB interface) and the surfaces examined were those of the solder remaining on the PCB.

In the as-assembled condition, the SnPb joint exhibits classic ductile dimple fracture, with dimples on the order of 10 – 30 μm across. The Pb-free joints, which have higher strength and toughness, exhibited a macroscopically flatter fracture surface than that of the SnPb joint, with small-scale roughness, Fig. 12. Similarly flat fracture surfaces were

observed by Sundelin et al. [5] in Pb-free QFP joints plated with Ni/Au/Pd and soldered onto Ni/Au-coated PCBs. The SAC/Sn joint, which had the highest strength, shows areas that are quite flat between areas with a rougher appearance. The SAC/SnBi joint fracture surface shows similar flat and rough areas but on a somewhat finer scale. Also evident was significant voiding for the SAC/SnBi joint. SAC solder joints are well known to exhibit substantial voiding. It is not clear whether voiding in the SAC/SnBi joint examined was present in all the Sn-Bi plated joints and whether voiding contributed to phenomena such as rapid growth and cracking of the IMC layer.
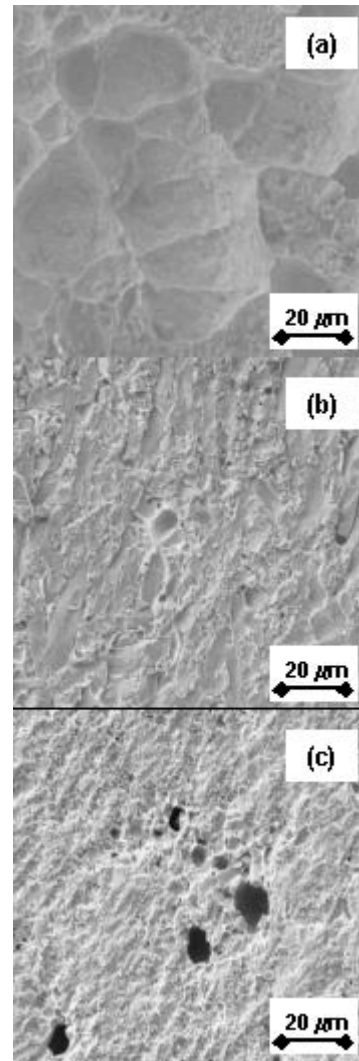
Figure 12. SEM fractographs following lead pull of as-assembled MQFP joints. (a) SnPb/SnPb, (b) SAC/Sn, (c) SAC/Sn3Bi.

Following aging at 150 °C for 8 days, the fracture surface of the Pb-free joints changed somewhat. Figure 13 shows an example for the SAC/Sn joint. Note the flatter appearance of the fracture surface compared to that for the as-assembled condition. Another feature of these fracture surfaces was a directional character. Note the "ridges" running vertically in Fig. 13. These features may be related to intermittent

"heel-to-toe" peeling of the joint at approximately constant load during fracture, which was common for this aging treatment.

Finally, following aging at 175 °C for 8 days the joints all failed at very low loads and displacements (Figs. 10 and 11). Figure 14 presents the fracture surface of a SAC/Sn joint with this aging treatment. Note the large, flat facets on the fracture surface, indicative of a brittle fracture. Such a fracture surface would be consistent with the thick intermetallic layer produced by such a severe aging, on the order of 10 μm or greater.

Thermal Fatigue Resistance of Leaded Packages
At the writing of this paper, 3185 accelerated thermal cycles of –40 to +125 °C are complete, and testing is still in progress. A much wider range of packages are being ATC tested than have been studied for aging and strength. In addition to the four types of MQFP joints described in previous sections of this paper, two other Sn-Bi lead plating compositions were included: Sn-1Bi and Sn-6Bi. Moreover, for the MQFP package type, samples with the various Pb-free lead platings are being tested with eutectic Sn-Pb solder to examine "backward compatibility" of the platings. In addition, the PLCC, TSOP and SOIC packages are being ATC tested.
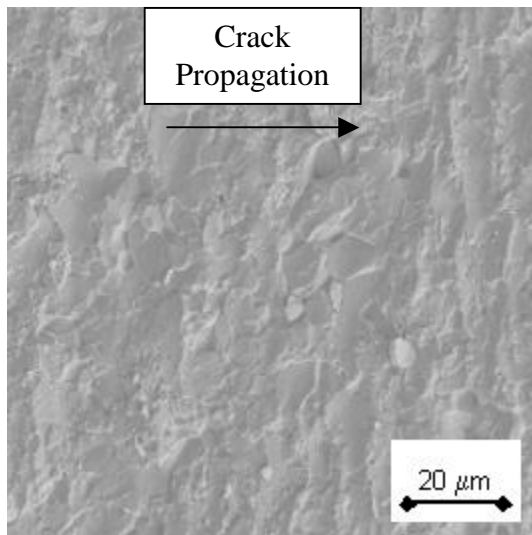

Figure 13. SEM fractograph for a SAC/Sn joint aged at 150 °C for 8 days.

Not enough failures have occurred following 3185 cycles to construct Weibull failure plots. The largest number of failures that have occurred are for MQFP packages with the Sn-Pb plating soldered to the PCB with the SAC solder. In this case, 4 of 18 packages have failed. For all other combinations of package type, solder alloy, and lead plating, either 0 or 1 failure has occurred. Although there are not enough data so far to make comparisons among the lead platings, package types, and solder alloys, it seems clear that thermal cycle reliability is not a major issue for the packages and joint metallurgies studied.
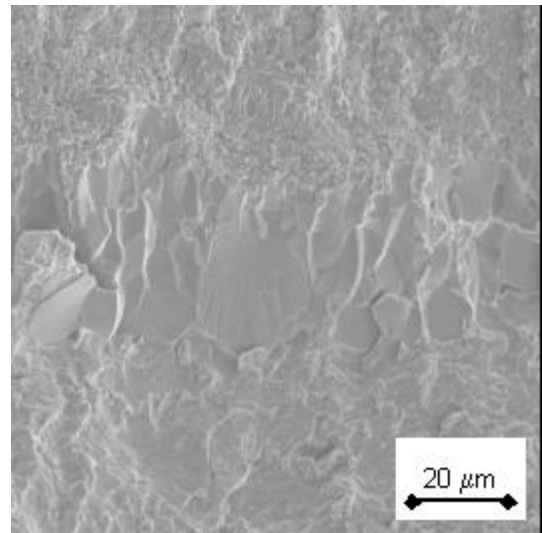
Figure 14. SEM fractograph for a SAC/Sn joint aged at 175 °C for 8 days.
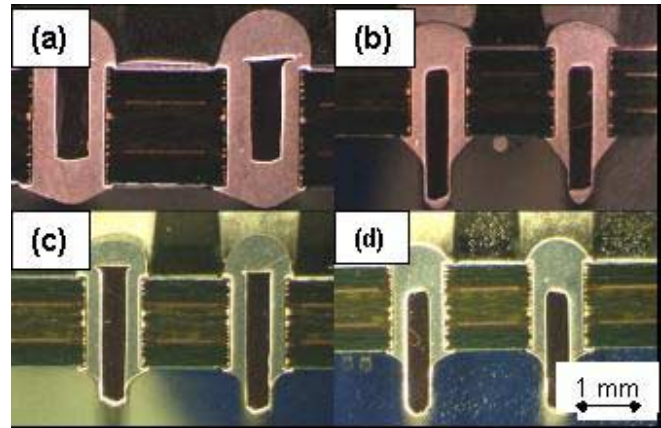
Figure 15. Cross sections of TH joints illustrating complete barrel fill for: (a) Sn-Pb/SnPb, (b) Sn-Pb/Sn-Bi, (c) SAC/Sn-Bi, (d) Sn-Cu/Sn-Bi joints.

Through-Hole Joint Evaluation
As stated in the Introduction, the focus of this limited study on through-hole (TH) joints was on barrel fill and wetting of the solder to the pins. The material combinations of solder/lead plating investigated include: Sn-Pb/Sn-3Bi, SAC/Sn-3Bi, Sn-Cu/Sn-3Bi, and Sn-Pb/Sn-Pb as a control.

Examination using optical microscopy revealed essentially complete filling of the barrel for all material combinations. This finding is illustrated by the cross-sections shown in Figure 15. Note the complete filling of the barrel, the lack of voids, and the clean interfaces between the solder and the leads and barrel. On the bottom side of the board, the pins were observed to be wet well by the solder, and the barrels were filled for all material combinations, as shown in Fig. 16 for Sn-Cu/Sn-Bi joints. On the top side of the board, full barrels were again observed as a general rule. Occasionally a barrel that was not 100% filled on the top side was

observed, but this was quite rare and not limited to a particular material combination. Furthermore, even in these cases the fill was well over 75%. For all material combinations, including Sn-Pb/Sn-Pb, the solder wet up some of leads while not on others on the same part. An example of this behavior is shown for Sn-Pb/Sn-Pb joints and for SAC/Sn-Bi joints in Fig. 17. It is commonly observed that TH joints with full barrels are not a reliability concern. Therefore, based on our observations, we see no evidence to suggest that any of the material combinations studied will result in unreliable TH joints.

SUMMARY AND CONCLUSIONS
SMT assemblies were made using Pb-free Sn-3.8Ag-0.7Cu solder and leaded components with surface finishes of: pure matte Sn, Sn-3Cu, and Sn alloyed with Bi in concentrations of 1, 3 and 6 weight percent. The impact of these finishes on the intermetallic layer growth during aging, strength, and thermal fatigue resistance of the solder joints was investigated. Furthermore, a limited study of wave soldered, plated through-hole joints was made for Sn-10Pb and Sn-3Bi lead finishes soldered with Sn-4.0Ag-0.5Cu and Sn-0.7Cu Pb-free solder alloys. Based on these experiments, the following conclusions have been made.

Figure 16. Wetting of the solder to the pins on the bottom side of a Sn-Cu/Sn-Bi PDIP assembly.

Growth of the $Cu_3Sn + Cu_6Sn_5$ layer at the interface between the copper PCB pad and the solder is slightly slower for the Pb-free joints than for conventional Sn-Pb joints, even though the initial layer thickness is slightly greater for the Pb-free joints. At the interface between the solder and the copper leads, only the Cu_6Sn_5 phase was observed. The growth of this layer varied depending on the lead plating alloy. For matte Sn and Sn-3Cu, growth was similar to that observed for Sn-Pb plated leads soldered with eutectic Sn-Pb solder paste, though the apparent activation energy appears to be somewhat greater for the Sn-3Cu plating. Joints with the Sn-3Bi plating exhibited an intermetallic growth rate and activation energy slightly larger than the other joints for moderate aging treatments. For severe aging conditions (e.g. 150 °C for 32 days and

175 °C for 8 days), growth became very rapid and thick, cracked intermetallic layers at the lead/solder interface were observed. Except in these cases, the growth of the intermetallic layers, both at the PCB and lead interfaces, followed a parabolic growth law. Further study is warranted to understand why the growth rate and activation energy for growth of the intermetallic is higher for the Sn-Bi plated leads than for the others platings.
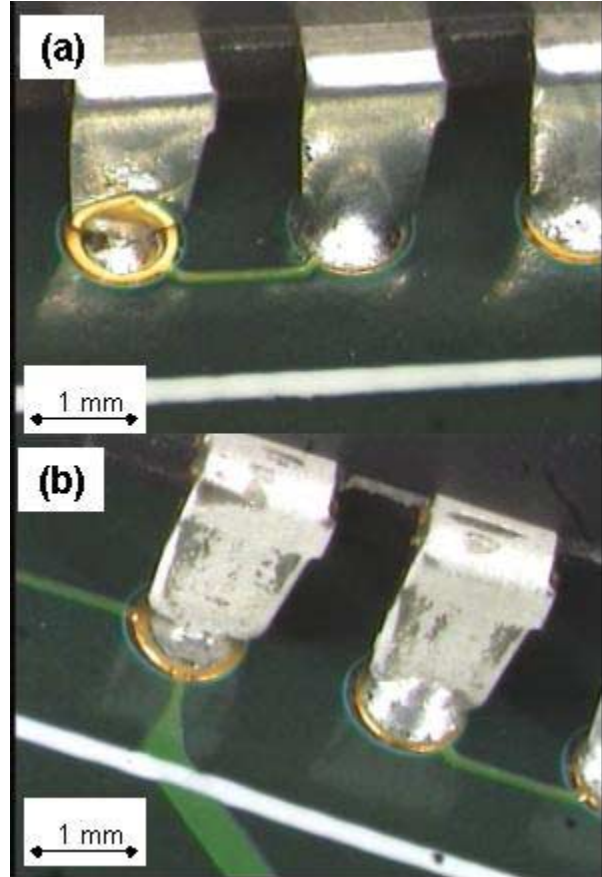
Figure 17. Barrel fill and lead wetting on the top side of (a) Sn-Pb/Sn-Pb and (b) SAC/Sn-Bi PDIP assemblies.

The strength and toughness of the Pb-free joints is greater than or equal to that of conventional Sn-Pb joints for all of the terminal finishes studied. Furthermore, the strength and toughness values are essentially maintained for aging treatments that result in a lead/solder IMC layer thickness of 4.5 to 7 μm, compared to an initial thickness of 2 to 3 μm. For severe aging treatments resulting in IMC layers of about 10 μm or more (150 °C for 32 days and 175 °C for 8 days), the strength and ductility of all joints becomes significantly degraded and the fractures become brittle in appearance. Such conditions are unlikely to occur in service. Thus, based on these findings, it appears that any of the Pb-free terminal finishes will produce joints with Sn-Ag-Cu solder that have room temperature strength and toughness values at least as good as conventional Sn-Pb joints, even after aging in service. The high IMC growth rates in the Sn-Bi plated leads under severe aging conditions may warrant further study, however, to confirm this conclusion.

Few, if any, failures have been produced by accelerated thermal cycling using a 60-minute, –40 and +125 °C profile up to 3185 cycles. These findings suggest that it is unlikely any of the lead plating alloys will result in thermal fatigue resistance problems. Of course, more data are required to make firm conclusions and to compare the thermal fatigue resistance resulting from the different terminal finishes.

The limited study conducted on barrel fill and wetting of PDIP components suggests that through-hole joints of adequate shape and appearance can be made using any of the material combinations (solder/lead plating) studied: Sn-Pb/Sn-3Bi, Sn-4.0Ag-0.5Cu/Sn-3Bi, Sn-0.7Cu/Sn-3Bi. It is commonly observed that TH joints with full barrels are not a reliability concern. Therefore, we see no evidence to suggest that any of the material combinations studied will result in unreliable TH joints. Additional studies are warranted to confirm this finding due to the limited scope of the current investigation.

REFERENCES
[1] P. Roubaud, et al., "Impact of Intermetallic Growth on the Mechanical Strength of Pb-Free BGA Assemblies," Proceedings of APEX, 2001, pp. LF2-3.
[2] T. Y. Lee, et al., "Morphology, Kinetics, and Thermodynamics of Solid State Aging of Eutectic SnPb and Pb-Free Solders ($SnAg_{3.5}$, $SnAg_{3.8}Cu_{0.7}$ and $SnCu_{0.7}$) on Cu, J. Materials Research, 2002, 17, 2 pp.291-301.
[3] P.T. Vianco, K.L. Erickson, and P.L. Hopkins, "Solid State Intermetallic Compound Growth Between Copper and High Temperature, Tin-Rich Solders – Part I: Experimental Analysis," J. Electronic Materials, 1994, 23, 8, pp. 721-727.
[4] E. Benedetto "Solderability and Board Level Reliability of Palladium Plated, Fine Pitch Components," Proceedings of Surface Mount International, 1998, pp. 624-631.
[5] J.J. Sundelin, et al., "Pull Testing of Lead-Free QFP Solder Joints," Proceedings of Electronic Components and Technology Conference, 2002, pp. 1622-1626.
[6] V. Schroeder, unpublished work, Hewlett-Packard Co., 2002.